Downloaded from http://iranpaper.ir
http://www.itrans24.com/landing1.html
سفارش ترجمه این مقاله
آنلاین: www.trans24.ir
تماس: ۶۶۵۷۲۲۳۸-۴۰ (۰۲۱)
trans24

Electrical Power and Energy Systems 75 (2016) 8–18

Contents lists available at ScienceDirect

Electrical Power and Energy Systems

journal homepage: www.elsevier.com/locate/ijepes

Analysis and compensation of voltage unbalance of a DFIG using predictive rotor current control

Van-Tung Phan [a,*], Thillainathan Logenthiran [a], Wai Lok Woo [a], Dave Atkinson [b], Volker Pickert [b]

[a] School of Electrical and Electronic Engineering, Newcastle University (Singapore campus), 172A Ang Mo Kio Avenue 8, #05-01, Singapore 567739, Singapore
[b] School of Electrical and Electronic Engineering, Newcastle University, Newcastle upon Tyne NE1 7RU, UK

ARTICLE INFO

Article history:
Received 27 July 2014
Received in revised form 30 April 2015
Accepted 28 August 2015
Available online 8 September 2015

Keywords:
Doubly fed induction generator
Predictive current control
Wind turbine
Unbalanced load
Stand-alone DFIG
Voltage unbalance

ABSTRACT

This paper analyzes the unbalance problem of a stand-alone doubly-fed induction generator (DFIG) under unbalanced loads and proposes a compensation method to balance the stator output voltage. The proposed compensation method is developed based on a predictive current control (PCC) method implemented in the rotor current controller. The development of the PCC is based on the discrete model of the DFIG to predict an appropriate average rotor voltage vector to eliminate the rotor current error in the following switching period. The identified rotor voltage vector is then applied to the rotor-side converter (RSC) by using space-vector modulation (SVM) with constant switching frequency. To improve the control performance, a compensation method for time delay based on the prediction of the future rotor current at the end of current sampling period also is investigated. The proposed control scheme was tested by experiments with 2.2 kW DFIG to demonstrate its excellent steady-state performance as well as extremely fast dynamic response.

© 2015 Elsevier Ltd. All rights reserved.

Introduction

Doubly fed induction generators (DFIGs) have been commonly used in variable-speed wind turbines [1–25] due to its advantages such as converters with slip rating, ease of implementation, and four-quadrant active and reactive power control. The control and operation of the DFIG have been focused on generator modeling [1–3], direct power control [3–10], fault ride-through capability [11–14], unbalanced grid voltage [6–10,15–16], and unbalanced load in case of stand-alone mode [17–25]. In these studies, the majority of current control systems for DFIG systems have been mainly developed based on the traditional vector control scheme using a conventional proportional-integral (PI) controller to regulate the current. However, it has major disadvantages such as steady-state errors, difficult tuning process of control parameters, and sensitivity to system parameters when reference control variables are not dc components. Consequently, this considerably reduces the control bandwidth and seriously causes oscillations on the control system in either the steady state or the transient behavior. Especially, the DFIG-based wind turbines working under unbalanced grid or unbalanced load conditions requires more accurate control due to the effect of the negative sequence component. Under such condition, control quantities are composed of the negative component with twice synchronous frequency that a conventional PI controller cannot regulate precisely. In order to increase the control accuracy, the analysis and operation of grid-connected DFIG systems under unbalanced network [6–10] or unbalanced stand-alone systems [17–25] have been widely investigated based on a dual rotating reference frame, called positive and negative frames. In this control approach, the positive and negative sequence components of the current are controlled in the positive and negative reference frames, respectively. However, these control schemes are too complicated to implement due to decomposition processes and frame transformations, which significantly increase the control time delay. To tackle this problem, an improved control approach for an unbalanced stand-alone DFIG system, implemented in a single positive reference frame with a PI plus a resonant controller (PIR), was introduced in [23,38]. The complexity in calculations of the control algorithm was greatly reduced, but the design of controller parameters was not a straightforward task. Furthermore, the transient performance of the proposed method was not taken into account in that research. As such, it is necessary to offer an optimal controller that gives faster transient response than PI and PIR controllers under unbalanced operating conditions for the DFIG system.

* Corresponding author. Tel.: +65 6908 6068.
E-mail addresses: vantung.phan@ncl.ac.uk (V.-T. Phan), t.logenthiran@ncl.ac.uk (T. Logenthiran), lok.woo@ncl.ac.uk (W.L. Woo), dave.atkinson@ncl.ac.uk (D. Atkinson), volker.pickert@ncl.ac.uk (V. Pickert).

http://dx.doi.org/10.1016/j.ijepes.2015.08.020
0142-0615/© 2015 Elsevier Ltd. All rights reserved.

Downloaded from http://iranpaper.ir
http://www.itrans24.com/landing1.html
سفارش ترجمه این مقاله
آنلاین: www.trans24.ir
تماس: ۶۶۵۷۲۲۳۸-۴۰ (۰۲۱)
trans24

Nomenclature

v_s, v_r	stator and rotor voltages
v_p	voltage at the point of common stator (PCS)
i_s, i_r, i_{ms}	stator current, rotor current and stator magnetizing current
λ_r	rotor flux
L_m	mutual inductance
R_r, L_r, L_s	rotor resistance, rotor inductance and stator inductance
ω_s, ω_r, ω_{sl}	synchronous, rotational rotor, and slip speeds
θ_s, θ_r, θ_{sl}	synchronous, rotational rotor, and slip angles
σ	total leakage factor
d/dt, Δ	differential operators in time domain and discrete time domain, respectively
ε	error values

Superscripts

+, −	synchronous positive and negative reference frames
$\wedge$, *	predicted and reference values

Subscripts

+, −	positive and negative sequence component
s, r	stator, rotor
dq	synchronous dq axes

Many developments of predictive current control (PCC) approach in the literature have shown very good performance for control of power converters and motor drives, offering the potential for obtaining fast transient response, null steady state errors, high control bandwidth, and accurate control. An overview of basic concepts, operating principles, and control diagrams of model predictive control for the traditional 3-phase voltage-source inverter was presented in [26]. For current controllers, the authors in [27] proposed a PCC method in which the future current values in the stationary reference frame were predicted with all possible switching states and then an optimal one that gave the minimum current error was chosen. The advantage of this PCC was no coupling effects between current responses when one of these reference currents was changed. However, the method to choose an optimal quality function utilizing constraints is difficult and sensitive. In [28], an enhanced predictive current control technique with fixed switching frequency was developed for an asymmetrical dual three-phase ac drive in which fast torque and current responses were achieved. The predictive control scheme helps avoid the use of PI controllers and pulse width modulation (PWM) schemes which are not easy to regulate controller gains in multiphase drives. A discrete-time PCC for a PMSM was proposed in [29], where a delay compensation method was employed by adopting a predictive observer for the current. However, the control algorithm is sensitive to machine parameters. In [30], a robust PCC method combining two-sample deadbeat control with a Luenberger observer was developed to estimate the future value of the grid current. However, the control algorithm requires more computational complexity. One of important characteristics of PCC method is the accuracy of estimated parameters of system models that significantly improve control performances. In [31], an online parameter estimation method with respect to PCC approach for a phase-controlled rectifier was outlined. A robust high bandwidth discrete-time PCC scheme for voltage-source PWM converters was developed in [32], where the time delay compensation method utilized a predictive current observer with an adaptive internal model for system uncertainties and disturbances. In addition, the PCC strategy has been proposed for microgrid applications [33], induction motor drives [34], inverters of uninterruptible power supply applications [35], active power filters [36], etc. However, it has been rare to see the PCC approach in DFIG applications.

The purpose of this paper is to develop an improved predictive rotor current control scheme for a stand-alone DFIG system connected to an unbalanced three-phase load. Under this working condition, the stator output voltage will be unbalanced due to the load effect and can be compensated by generating a proper reference rotor current for the rotor current controller. Due to the requirement for controlling the ac terms of both positive and negative sequence components in the reference rotor current during voltage unbalance, the proposed predictive rotor current control scheme was developed to improve the current control accuracy and to increase the control bandwidth and system stability. The principle of the proposed PCC method is to predict the appropriate average rotor voltage vector in the next sampling period in order to remove the rotor current error in the next sampling period. To enhance the control accuracy and improve control performance, a conceptual analysis of PCC with the control time delay compensation for such a DFIG system is clearly analyzed and effectively implemented. The control time delay compensation method in which the sampling frequency is set as two times of PWM switching frequency is developed to accurately predict the actual instantaneous values of the rotor current, which greatly enhance the control performance. The whole control scheme is based on the positive reference frame where there is no need sequential decomposition of the measured rotor current. The paper is organized as follows. Section 'Unbalance problem in an unbalanced stand-alone DFIG' analyzes the unbalance problems in an unbalanced stand-alone DFIG system. The proposed PCC algorithm under unbalanced operation conditions is discussed in Section 'The proposed PCC algorithm of DFIG control scheme'. Next, Section 'Experimental results' will show experimental results to demonstrate the advanced features of the proposed PCC control scheme. The conclusions are drawn in Section 'Conclusions'.

Unbalance problem in an unbalanced stand-alone DFIG

Analysis of unbalanced stator voltage of DFIG

Fig. 1 shows the general configuration of a stand-alone DFIG supplying an unbalanced three-phase load. The system is composed of a rotor-side converter and a load-side converter (LSC),

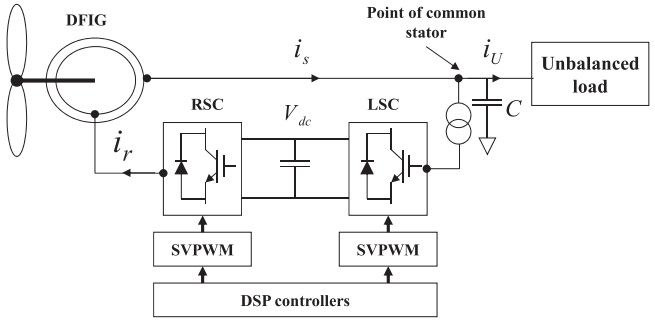

Fig. 1. Back-to-back converters based DFIG configuration with an unbalanced load.

Downloaded from http://iranpaper.ir
http://www.itrans24.com/landing1.html
سفارش ترجمه این مقاله
آنلاین: www.trans24.ir
تماس: ۶۶۵۷۲۲۳۸-۴۰ (۰۲۱)
trans24

and both of them are controlled by the digital DSP controllers. A capacitor is connected to the stator terminal as a filter. The unbalanced loads can be two cases: one phase load impedance unequal to two remaining ones, and three unequal load impedances. In this paper, the unbalanced load is modeled as a Y-connected three phase load. These unbalanced loads regularly cause unbalanced three-phase voltage at the point of common stator (PCS). If such voltage unbalance is not taken into account, it seriously reduces the quality of stator voltage of the DFIG. The main reason to produce the voltage unbalance at the PCS is the effect of the unbalanced load current, drawn by the unbalanced load. Therefore, the elimination of this voltage unbalance is an essential task to improve the voltage quality of the stand-alone DFIG generator.

Fig. 2 shows the connection interface between the DFIG and different load types connected to the stator terminals. R_s and L_s are the stator resistance and inductance of the DFIG and are considered as the internal impedance of the DFIG. As seen, the presence of the unbalanced load directly causes unbalance on the stator voltage at the PCS, which deteriorates the performance of other loads connected at this point of the DFIG. This can be explained that the unbalanced load current (i_U) leads to an unbalanced drop voltage (v_U) on the internal stator impedance including both the positive and negative sequence components. The voltage at the PCS is determined as

$$v_P = v_s - v_U = v_s - R_s i_s - L_s \frac{di_s}{dt} \tag{1}$$

Taking into account both the positive and negative sequence components, Eq. (1) yields

$$v_P = \left(v_s - R_s i_{s+} - L_s \frac{di_{s+}}{dt}\right) - \left(R_s i_{s-} + L_s \frac{di_{s-}}{dt}\right) \tag{2}$$

where the positive sequence voltage at the PCS is

$$v_{P+} = v_s - R_s i_{s+} - L_s \frac{di_{s+}}{dt} \tag{3}$$

and the negative sequence voltage is determined as

$$v_{P-} = -R_s i_{s-} - L_s \frac{di_{s-}}{dt} \tag{4}$$

Accordingly, despite of balanced stator voltage (v_s), the voltage at the PCS is an unbalanced waveform due to the unbalanced voltage (v_U). Generally, a stand-alone DFIG system is controlled by inverter interfaces in which the inverter can be controlled to produce a desired output voltage (v_s) to balance the voltage at the PCS. Therefore, this paper deals with unbalance compensation method for the DFIG under such operation conditions, which is based on the PCC algorithm in the RSC. The purpose of this proposed controller is to generate a stator voltage (v_s) with the negative sequence component in order to cancel the unbalanced voltage drop (v_U). As a result, a balanced voltage waveform can be produced at the PCS.

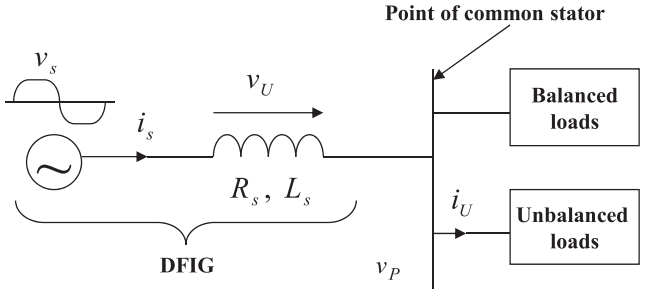

Fig. 2. Connection interface between the DFIG and different load types at the point of common stator.

Voltage unbalanced factor

The effect of stator voltage unbalance under unbalanced load conditions can be severe on the generator and power electronic converters, causing more losses and heating effects. To assess such adverse effects, the "true" voltage unbalance factor (UF) for three-phase sinusoidal voltage waveforms is presented in [37]. According to this, the UF is defined as

$$\mathrm{UF}(\%) = \frac{V_-}{V_+} \times 100\% \tag{5}$$

where V_+ and V_- are the modulus of the root mean square (RMS) of the positive and negative sequence components, respectively. These components are calculated based on only RMS values of the line voltages, which are possible to measure with voltage meters. They are given as follows

$$V_+ = \sqrt{\frac{A_m^2 + \frac{4A_s^2}{\sqrt{3}}}{2}}, \quad V_- = \sqrt{\frac{A_m^2 - \frac{4A_s^2}{\sqrt{3}}}{2}} \tag{6}$$

$$A_m^2 = \frac{V_{AB}^2 + V_{BC}^2 + V_{CA}^2}{3} \tag{7}$$

$$A_s^2 = \sqrt{p(p - V_{AB})(p - V_{BC})(p - V_{CA})} \tag{8}$$

$$p = \frac{V_{AB} + V_{BC} + V_{CA}}{3} \tag{9}$$

The proposed PCC algorithm of DFIG control scheme

Dynamic DFIG model and reference frame

Under the unbalanced load condition in stand-alone DFIG systems, the most popular method to analyze the DFIG model is to use the positive reference frame rotating at the speed ω_s and the negative reference frame rotating at the speed $-\omega_s$. Fig. 3 shows a vector diagram that represents the relationship between the stationary frame $\alpha_s\beta_s$, the rotor frame $\alpha_r\beta_r$ rotating with an angular speed ω_r, the positive frame dq^+ rotating with an angular speed ω_s, and the negative frame dq^- rotating with an angular speed $-\omega_s$ is used. The superscripts + and − represent the positive and negative synchronous reference frames, respectively. The vector F denotes the values of the voltage, current, or flux in the stator voltage-oriented reference frame. The relationship of vector F between different frames is illustrated as follows

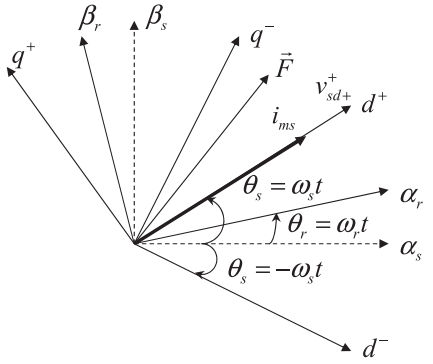

Fig. 3. Vector diagram of various reference frames used in the PCC control scheme.

Downloaded from http://iranpaper.ir
http://www.itrans24.com/landing1.html
سفارش ترجمه این مقاله
آنلاین: www.trans24.ir
تماس: ۶۶۵۷۲۲۳۸-۴۰ (۰۲۱)
trans24

$$F_{dq}^{+} = F_{\alpha_s\beta_s} e^{-j\omega_s t} = F_{dq}^{-} e^{-j2\omega_s t}$$
$$F_{dq}^{-} = F_{\alpha_s\beta_s} e^{j\omega_s t} = F_{dq}^{+} e^{j2\omega_s t} \quad (10)$$

Taking into account the control system in the single positive reference frame only, the vector F can be expressed by

$$F_{dq}^{+} = F_{dq+}^{+} + F_{dq-}^{-} = F_{dq+}^{+} + F_{dq-}^{-} e^{-j2\omega_s t} \quad (11)$$

where the subscripts + and − represent the positive and negative sequence components, respectively.

Since the PCC method is developed based on the analysis of rotor voltages and stator, rotor fluxes, it is important to show the relation of these components. The rotor fluxes λ_{rdq}^{+} and the rotor voltages v_{rdq}^{+} in the positive synchronous reference frame rotating at angular speed ω_s are given by

$$\lambda_{rd}^{+} = L_r i_{rd}^{+} + L_m i_{sd}^{+} = \frac{L_m^2}{L_s} i_{ms} + \sigma L_r i_{rd}^{+} \quad (12)$$

$$\lambda_{rq}^{+} = L_r i_{rq}^{+} + L_m i_{sq}^{+} = \sigma L_r i_{rq}^{+} \quad (13)$$

$$v_{rd}^{+} = R_r i_{rd}^{+} + \sigma L_r \frac{d}{dt} i_{rd}^{+} - \omega_{sl}^{+} \sigma L_r i_{rq}^{+} \quad (14)$$

$$v_{rq}^{+} = R_r i_{rq}^{+} + \sigma L_r \frac{d}{dt} i_{rq}^{+} + \omega_{sl}^{+} \left(\frac{L_m^2}{L_s} i_{ms} + \sigma L_r i_{rd}^{+} \right) \quad (15)$$

where R_r, L_m, L_r, L_s, σ, i_{ms} are the nominal values of rotor resistance, mutual inductance, rotor inductance, stator inductance, total leakage factor, and stator magnetizing current of the generator, respectively. $\omega_{sl}^{+} = \omega_s - \omega_r$ is the slip speed of generator in the positive rotating reference frame. In addition, i_{rd}^{+}, i_{rq}^{+}, i_{sd}^{+}, and i_{sq}^{+} are the dq axis rotor and stator currents in the positive reference frame as well, respectively.

Compensation of unbalanced stator voltage and generation of reference rotor current

As analyzed in Section 'Unbalance problem in an unbalanced stand-alone DFIG', the control scheme is responsible for producing a proper stator voltage (v_s) with the negative sequence component in order to cancel the unbalanced voltage drop (v_U). In order to do this task, the negative sequence components of the stator voltage at the PCS must be detected and compensated. First, notch filters are adopted to extract the negative sequence of the voltage, i.e., v_{Pd-}^{-} and v_{Pq-}^{-}. Next, to eliminate these components completely, two PI voltage controllers are used in which the reference values are set zero, as seen in Fig. 4. The outputs of these controllers are the reference negative sequence components of rotor currents, i.e., i_{rd-}^{-} and i_{rq-}^{-}. Therefore, the reference rotor current for the PCC algorithm is the sum of both ac and dc components, calculated by (16) and (17). It should be noted that the frequency of the ac component in the reference rotor current is twice synchronous frequency.

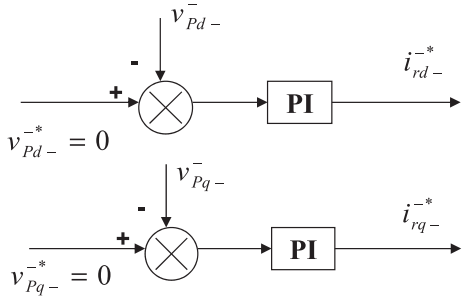

Fig. 4. Four PI controllers based voltage control loop to eliminate the negative sequence voltage components.

$$i_{rd}^{+*} = i_{rd+}^{+*} + i_{rd-}^{+*} = i_{rd+}^{+*} + i_{rd-}^{-*} e^{-j2\theta_s} \quad (16)$$

$$i_{rq}^{+*} = i_{rq+}^{+*} + i_{rq-}^{+*} = i_{rq+}^{+*} + i_{rq-}^{-*} e^{-j2\theta_s} \quad (17)$$

Once these reference rotor currents are regulated adequately by the proposed rotor current controller, a corresponding induced stator voltage with the negative sequence will be generated to satisfy the desired control target.

PCC algorithm for an unbalanced stand-alone DFIG

The main objective of the PCC method in a DFIG system is to force the rotor output current follow the reference rotor current in (16) and (17). In this work, the reference rotor current is generated by an outer voltage control loop and a negative sequence component, added to compensate for stator voltage unbalances. Therefore, the dynamic rotor current under unbalanced operating conditions that consists of both the positive and negative sequence components, can be represented by the following equations

$$\frac{di_{rd}^{+}}{dt} = -\frac{R_r}{\sigma L_r} i_{rd}^{+} + \frac{v_{rd}^{+}}{\sigma L_r} + \omega_{sl} i_{rq}^{+} \quad (18)$$

$$\frac{di_{rq}^{+}}{dt} = -\frac{R_r}{\sigma L_r} i_{rq}^{+} + \frac{v_{rq}^{+}}{\sigma L_r} - \omega_{sl} i_{rd}^{+} - \omega_{sl} \frac{L_m^2}{\sigma L_r L_s} i_{ms} \quad (19)$$

For digital implementation of the PCC, the equations in (18) and (19) can be transformed into discrete time domain with a relatively small sampling time period T_s. As seen in (20) and (21), the derivative of the rotor current in the following sampling period can be estimated based on the current values and the system model.

$$\Delta i_{rd}^{+}(k) = -\frac{T_s R_r}{\sigma L_r} i_{rd}^{+}(k) + \frac{T_s v_{rd}^{+}}{\sigma L_r} + T_s \omega_{sl}(k) i_{rq}^{+}(k) \quad (20)$$

$$\Delta i_{rq}^{+}(k) = -\frac{T_s R_r}{\sigma L_r} i_{rq}^{+}(k) + \frac{T_s v_{rq}^{+}}{\sigma L_r} - T_s \omega_{sl}(k) \left(i_{rd}^{+}(k) + \frac{L_m^2}{\sigma L_r L_s} i_{ms}(k) \right) \quad (21)$$

The proposed PCC for an unbalanced DFIG system is constructed based on the model of the DFIG generator. In order to regulate the output rotor current to follow its reference at the end of the next switching period, the average required output rotor voltages $\bar{v}_{rdq}^{+}(k)$ should be precisely predicted in the next switching period; and they are shown in the discrete platform as (22) and (23). These predicted rotor voltages are then applied into the RSC to force the rotor current error to zero. To increase the control performance in terms of low distortion and low current ripple, the required rotor voltage is then controlled using SVPWM technique.

$$\bar{v}_{rd}^{+}(k) = R_r i_{rd}^{+}(k) + \frac{\sigma L_r}{T_s} \Delta i_{rd}^{+}(k) - \omega_{sl} \sigma L_r i_{rq}^{+}(k) \quad (22)$$

$$\bar{v}_{rq}^{+}(k) = R_r i_{rq}^{+}(k) + \frac{\sigma L_r}{T_s} \Delta i_{rq}^{+}(k) + \omega_{sl}(k) \left(\frac{L_m^2}{L_s} i_{ms}(k) + \sigma L_r i_{rd}^{+}(k) \right) \quad (23)$$

From equations above, it can be seen that the derivative of the rotor current is determined from two successive sampling instant values, given as

$$\Delta i_{rdq}^{+}(k) = i_{rdq}^{+}(k+1) - i_{rdq}^{+}(k) \quad (24)$$

According to (22)–(24), the control rotor voltages can be calculated with the measured quantities of the rotor current at kth and the predicted quantities at $(k+1)$th switching period. As

Downloaded from http://iranpaper.ir
http://www.itrans24.com/landing1.html
سفارش ترجمه این مقاله
آنلاین: www.trans24.ir
تماس: ۶۶۵۷۲۲۳۸-۴۰ (۰۲۱)
trans24

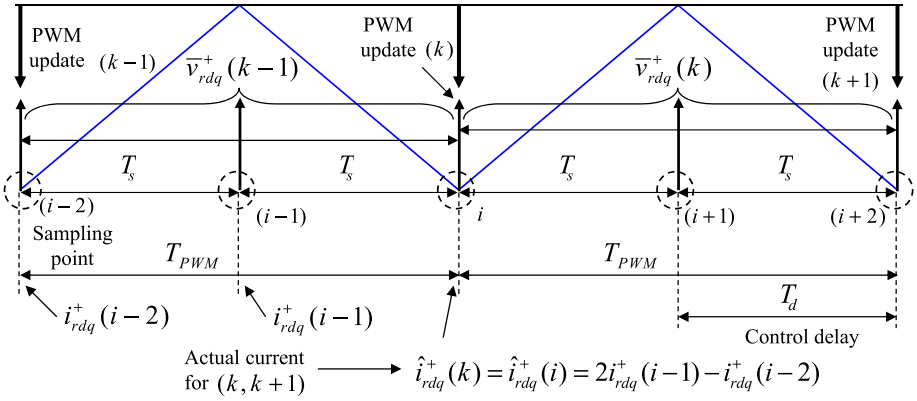

Fig. 5. Proposed sampling method and PWM update in the proposed PCC.

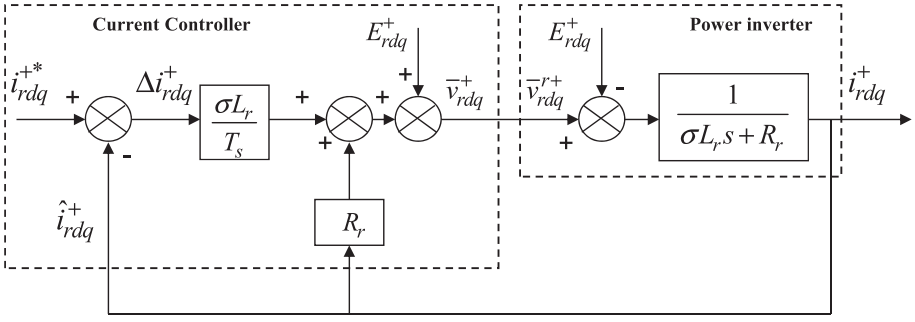

Fig. 6. Block diagram of the proposed current controller in the RSC.

addressed, the purpose of the PCC is to eliminate the rotor current error $\varepsilon i^{+}_{rdq}(k+1)$ at the end of the next switching period $(k+1)$th. It means that the control algorithm has to satisfy the following control target

$$\varepsilon i^{+}_{rdq}(k+1) = i^{+*}_{rdq}(k+1) - i^{+}_{rdq}(k+1) = 0 \tag{25}$$

Hence, the derivative of the rotor current in (22) and (23) can be expressed as

$$\Delta i^{+}_{rdq}(k) = i^{+*}_{rdq}(k+1) - i^{+}_{rdq}(k) \tag{26}$$

The superscript '$*$' denotes the reference value. The predicted reference rotor current at $(k+1)$th can be linearly calculated using previous values by the simple extrapolation method. Consequently, the reference value at $(k+1)$th can be easily calculated as (27) by using first order sample

$$i^{+*}_{rdq}(k+1) = 2i^{+*}_{rdq}(k) - i^{+*}_{rdq}(k-1) \tag{27}$$

Thus, (26) results

$$\Delta i^{+}_{rdq}(k) = 2i^{+*}_{rdq}(k) - i^{+*}_{rdq}(k-1) - i^{+}_{rdq}(k) \tag{28}$$

Substituting (28) into (22) and (23), the average rotor control voltages can be calculated. However, these rotor voltages do not take into account the effect of the control time delay due to the sampling and calculation processes. Therefore, if such rotor voltages are directly adopted in the controller, the control algorithm can result in large overshoot and oscillations in the rotor current. To overcome this problem, a compensation method for such time delay should be employed.

Proposed prediction method of actual rotor current

As mentioned before, the proposed compensation method in PCC for the time delay issue is developed based on the fact that the sampling frequency is set as two times of PWM switching frequency. As seen in Fig. 5, the sampling process is synchronized with the beginning and midpoint of the space vector modulation (SVM) carrier waveform. As such, the control time delay is a half of the switching period. It should be noted that the calculation process is done only when the sampled value at sampling instant $(i-1)T_s$ (midpoint) is completed. The calculation process of the proposed control algorithm for the switching interval $[k, k+1]$ is executed during the previous switching interval $[k-1, k]$ using two previous sampled values for the rotor current prediction. The reason is that the measured rotor current $i^{+}_{rdq}(k)$ at $(i-1)T_s$ is different from the actual rotor current $\hat{i}^{+}_{rdq}(k)$ at iT_s, which is achieved with the required rotor voltage $\bar{v}^{+}_{rdq}(k)$ at kth to be applied to the inverter to take the effect on the rotor current response. In order to effectively compensate for such control time delay, it is necessary to predict the actual instantaneous rotor current values $\hat{i}^{+}_{rdq}(k)$ at the end of the current PWM switching interval $[k-1, k]$, which will be used for estimating the required rotor voltage vectors in the next sampling period. The measured rotor currents can be considered linear during each PWM cycle at sampling instants $(i-2)T_s$, $(i-1)T_s$, and iT_s, where zero voltage vectors are executed on the inverter. Therefore, using the simple linear extrapolation technique, the actual rotor current at the end of the current PWM period $[k-1, k]$ can be estimated for the precise measurements of rotor currents, given as

$$\hat{i}^{+}_{rdq}(k) = \hat{i}^{+}_{rdq}(i) = 2i^{+}_{rdq}(i-1) - i^{+}_{rdq}(i-2) \tag{29}$$

Downloaded from http://iranpaper.ir
http://www.itrans24.com/landing1.html
سفارش ترجمه این مقاله
آنلاین: www.trans24.ir
تماس: ۶۶۵۷۲۲۳۸-۴۰ (۰۲۱)
trans24

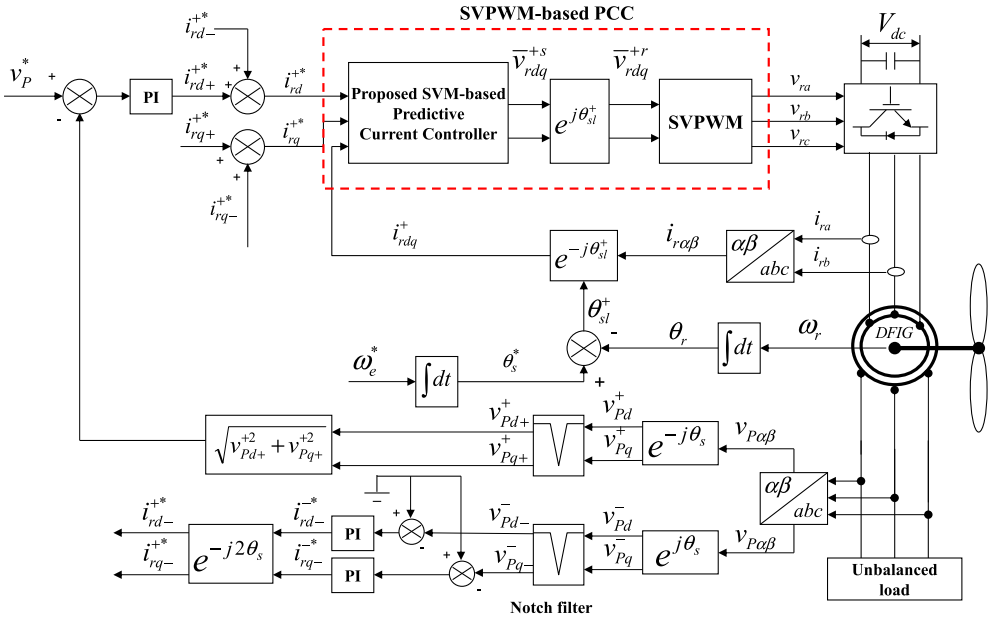

Fig. 7. Proposed current control scheme for the RSC of a DFIG under an unbalanced load.

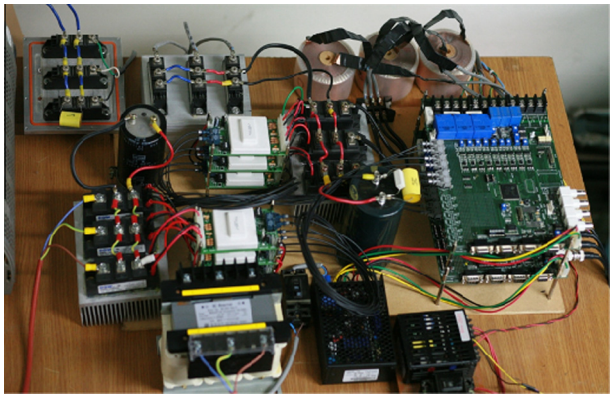

Fig. 8. Prototype of the experimental system.

Substituting (29) into (22), (23) and (28), the final average rotor voltages for the switching period $[k, k+1]$ can be calculated to obtain deadbeat predictive current control as follows

$$\bar{v}_{rd}^{+}(k) = R_r \hat{i}_{rd}^{+}(k) + \frac{\sigma L_r}{T_s}\Delta\hat{i}_{rd}^{+}(k) - \omega_{sl}\sigma L_r \hat{i}_{rq}^{+}(k) \tag{30}$$

$$\bar{v}_{rq}^{+}(k) = R_r \hat{i}_{rq}^{+}(k) + \frac{\sigma L_r}{T_s}\Delta\hat{i}_{rq}^{+}(k) + \omega_{sl}(k)\left(\frac{L_m^2}{L_s} i_{ms}(k) + \sigma L_r \hat{i}_{rd}^{+}(k)\right) \tag{31}$$

where $\Delta\hat{i}_{rdq}^{+}(k) = 2i_{rdq}^{+*}(k+1) - \hat{i}_{rdq}^{+}(k)$.

Because the modulation index of a doubly fed induction machine must be performed in the rotor-oriented reference frame, these obtained rotor voltages have to be transformed from synchronous frame to the rotor reference frame using an angular slip angle, given as

$$\bar{v}_{rdq}^{r+}(k) = \bar{v}_{rdq}^{+}(k)\, e^{j\theta_{sl}^{+}(k)} \tag{32}$$

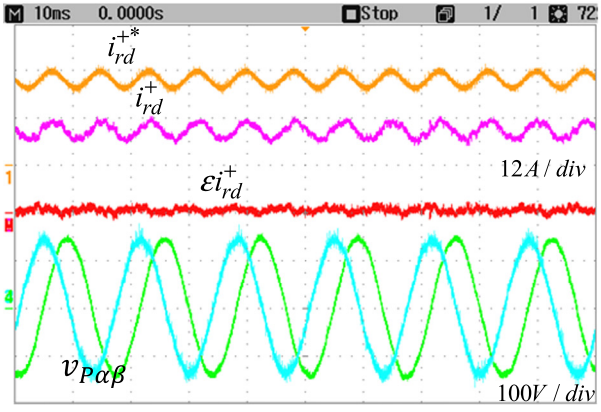

(a) Without time delay compensation

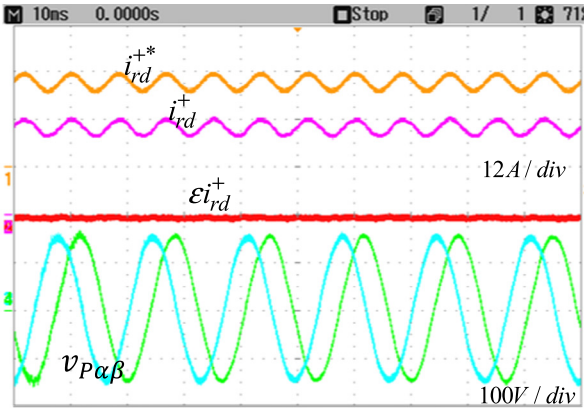

(b)With time delay compensation

Fig. 9. Experimental results of steady state performance of the PCC: (1) *d*-axis reference rotor current (i_{rd}^{+*}), (2) measured rotor current (i_{rd}^{+}), (M) rotor current error (εi_{rd}^{+}), (3–4) stator voltage at the PCS ($v_{P\alpha\beta}$).

Downloaded from http://iranpaper.ir
http://www.itrans24.com/landing1.html
سفارش ترجمه این مقاله
آنلاین: www.trans24.ir
تماس: ۶۶۵۷۲۲۳۸-۴۰ (۰۲۱)
trans24

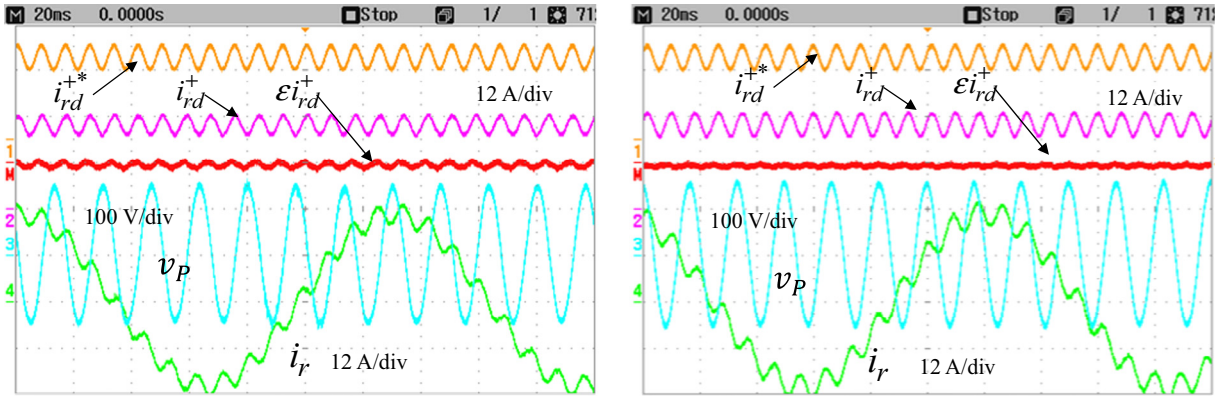

Fig. 10. Comparative experimental results of the steady state performance between PI controller (a) and the proposed PCC (b): (1) *d*-axis reference rotor current (i_{rd}^{+*}), (2) measured rotor current (i_{rd}^{+}), (M) rotor current error (εi_{rd}^{+*}), (3) phase stator voltage at the PCS (v_P), (4) phase rotor current (i_r).

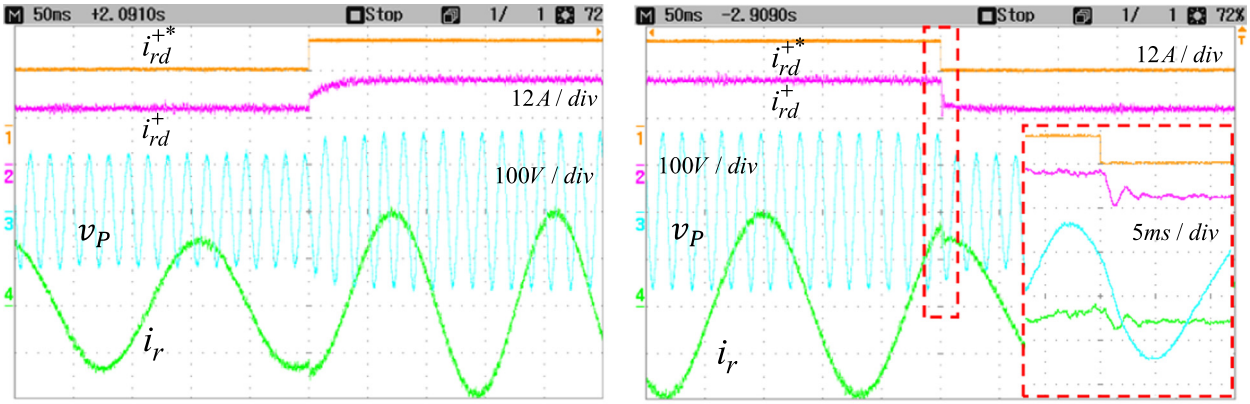

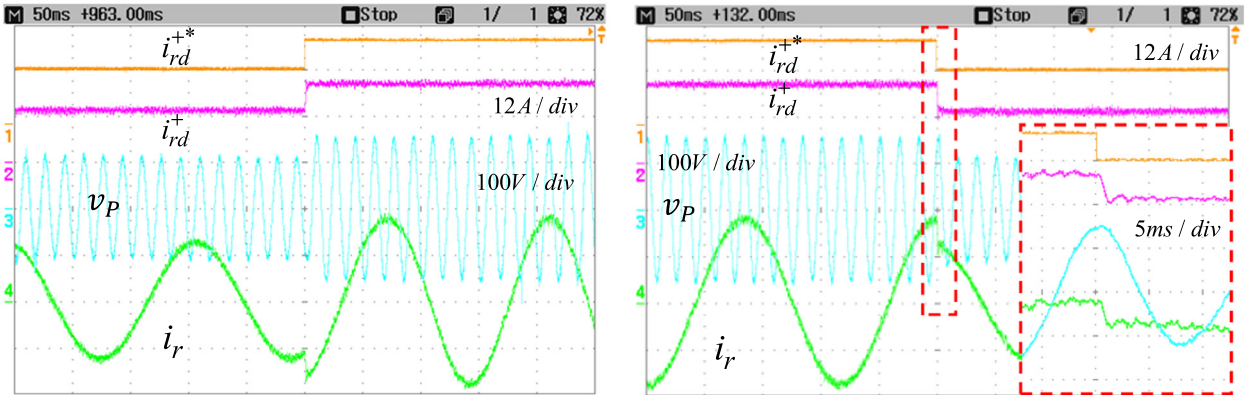

Fig. 11. Comparison of the dynamic performance between the PCC and the conventional PI controller under a balanced load: (1) *d*-axis reference rotor current (i_{rd}^{+*}), (2) measured rotor current (i_{rd}^{+}), (3) phase stator voltage at the PCS ($v_{P\alpha\beta}$), (4) phase rotor current (i_r).

Proposed control scheme with the DFIG

The block diagram of the proposed PCC is described in Fig. 6. E_{rdq}^{+} is equivalent to rotor back electromagnetic force acting as a disturbance to the PCC. Therefore, in the controller, this component is considered as a feed-forward input to cancel the rotor disturbance in the closed-loop.

The proposed block diagram of a stand-alone DFIG with the stator voltage compensation method is presented in Fig. 7. As can be seen, the stator voltage magnitude is controlled directly with a given specific command value v_P^* by adding an external voltage control loop. The magnitude of the stator voltage is obtained from the positive sequence components of the measured voltage signals, given as

Downloaded from http://iranpaper.ir
http://www.itrans24.com/landing1.html
سفارش ترجمه این مقاله
آنلاین: www.trans24.ir
تماس: ۶۶۵۷۲۲۳۸-۴۰ (۰۲۱)
trans24

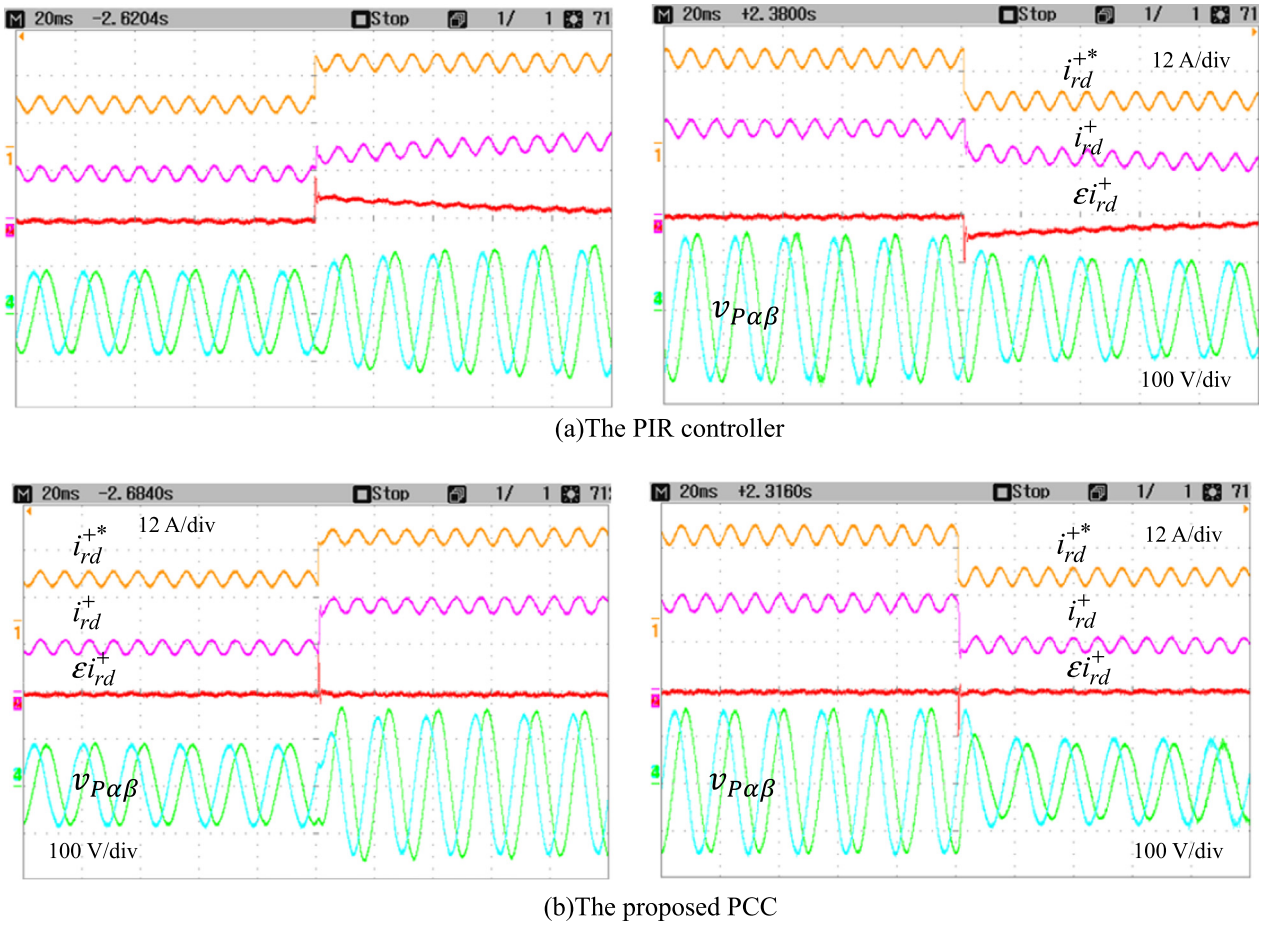

Fig. 12. Comparison of the dynamic performance between the PCC and the PIR controller [23] under an unbalanced load: (1) d-axis reference rotor current (i_{rd}^{+*}), (2) measured rotor current (i_{rd}^{+}), (M) rotor current error (εi_{rd}^{+}), (3–4) phase stator voltage at the PCS ($v_{P\alpha\beta}$).

$$v_P = \sqrt{v_{Pd+}^{+2} + v_{Pq+}^{+2}} \tag{33}$$

Under unbalanced load operation, the stator voltages in the positive rotating reference frame include both the dc and ac values at the double-frequency due to the presence of negative sequence components. In order to balance the stator output voltage imbalance, the negative sequence components must be eliminated by taking into account an appropriate control algorithm in the RSC. The proposed compensation method is implemented by adding the negative reference rotor currents in the current controller. Therefore, the total reference rotor current is the sum of both the dc and ac components, which are shown below

$$\begin{aligned} i_{rd}^{+*} &= i_{rd+}^{+*} + i_{rd-}^{+*} \\ i_{rq}^{+*} &= i_{rq+}^{+*} + i_{rq-}^{+*} \end{aligned} \tag{34}$$

where

$$\begin{aligned} i_{rd-}^{+*} &= i_{rd-}^{-*} e^{-j2\theta_s} \\ i_{rq-}^{+*} &= i_{rq-}^{-*} e^{-j2\theta_s} \end{aligned} \tag{35}$$

Experimental results

The experiment platform is setup in laboratory so as to implement the DFIG system and to verify the proposed control scheme. Experimental configuration is shown in Fig. 8. The system consists of a 2.2-kW DFIG, rotated by a DC motor that is emulated as a prime mover with the speed control. The RSC is fed by an IGBT-based PWM inverter in which the PWM switching frequency is 5 kHz and the sampling frequency is 10 kHz. The system is controlled with a high performance DSP TMS320F2812 of Texas Instrument. To test improved performance of the proposed PCC, the generator is tested under different operating conditions. The line to neutral voltage is controlled about 145 V. The synchronous frequency of the stator output voltage is controlled at 60 Hz. The unbalanced loads for the tests are approximately 10% in case of 30Ω, 40Ω, 50Ω. Each load subset is connected to one of the three-phase stator terminals A, B, or C.

Firstly, comparative results of the control scheme with and without control time delay compensation are presented. The steady state performance of the proposed PCC in the RSC for the unbalanced DFIG system is obtained with the rotor speed maintained constant at 1000 rpm whereas the synchronous speed of the generator is 1200 rpm. Fig. 9 shows the results of d-axis rotor current in the positive reference frame and the balanced stator voltages that are obtained with the proposed controller.

As can be seen, the d-axis rotor current consists of both the positive and negative sequence components with twice synchronous frequency (120 Hz). The role of the negative sequence rotor current is to induce an unbalanced stator voltage v_s. As a result, the stator voltage waveforms at the PCS are balanced well. For the PCC without time delay compensation shown in Fig. 9(a), the steady state tracking performance of the rotor current is significantly degraded due to the reduced control loop bandwidth. In contrast, Fig. 9(b) shows better results of the proposed PCC method in terms of zero

Downloaded from http://iranpaper.ir
http://www.itrans24.com/landing1.html
سفارش ترجمه این مقاله
آنلاین: www.trans24.ir
تماس: ۶۶۵۷۲۲۳۸-۴۰ (۰۲۱)
trans24

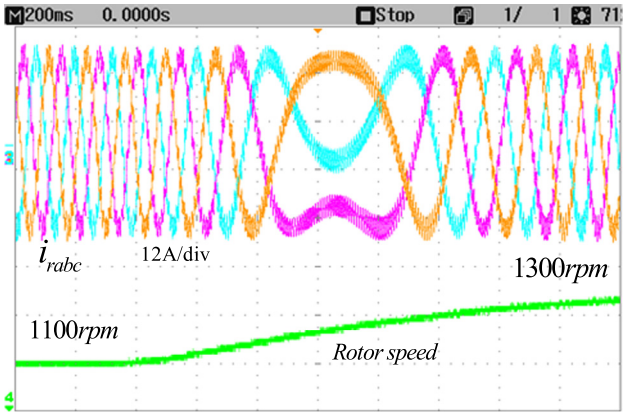

Fig. 13. Dynamic performance of the rotor current with varying rotor speed.

steady state error in rotor current and improved balanced stator voltage.

In addition, in order to approve more satisfactory performance of the proposed control scheme, Fig. 10 shows the experimental results to compare the steady state performance between the proposed PCC and the PI controller under the same conditions. Taking into account the error of the rotor current, Fig. 10 indicates that adequate and precise control of the current controller can be achieved with the proposed PCC approach in the positive synchronous reference frame. In contrast, the conventional PI controller results imprecise control with non-zero steady state error due to its insufficient control bandwidth.

Next, to verify the dynamic performance of the proposed PCC method, the tests are performed with the rotor current step changes, which are also done with a conventional PI controller in case of a balanced load and the PI-R controller in case of an unbalanced load. From Fig. 11, it can be seen with balanced loads that the proposed PCC method gives faster transient response and more robust performance when compared to the conventional PI current controller during the step changes of the *d*-axis rotor current. More clearly, Fig. 11(a) shows very low dynamic response of the PI controller with the raising time and falling time about 50 ms, whereas the proposed PCC method provides very fast transient behavior within a few milliseconds, no overshoot and oscillations, as seen in Fig. 11(b). The corresponding dynamic waveforms of the stator phase voltage and the rotor phase current with respect to step changes of *d*-axis rotor current are also shown in Fig. 11. It is observed that the PCC method offers more excellent transient performance than the PI controller under the same operating condition.

To further demonstrate the effectiveness of the proposed PCC, the same tests above implemented with an unbalanced load are shown in Fig. 12. This test is also performed with the PIR controller, as introduced in [23]. Under the unbalanced load condition, the rotor current contains two positive and negative components as indicated previously. From these figures, it can be observed that the transient response of the proposed PCC is also more rapid and effective than the case using the PIR controller. Taking into account the dynamic errors of the rotor current, Fig. 12(b) indicate

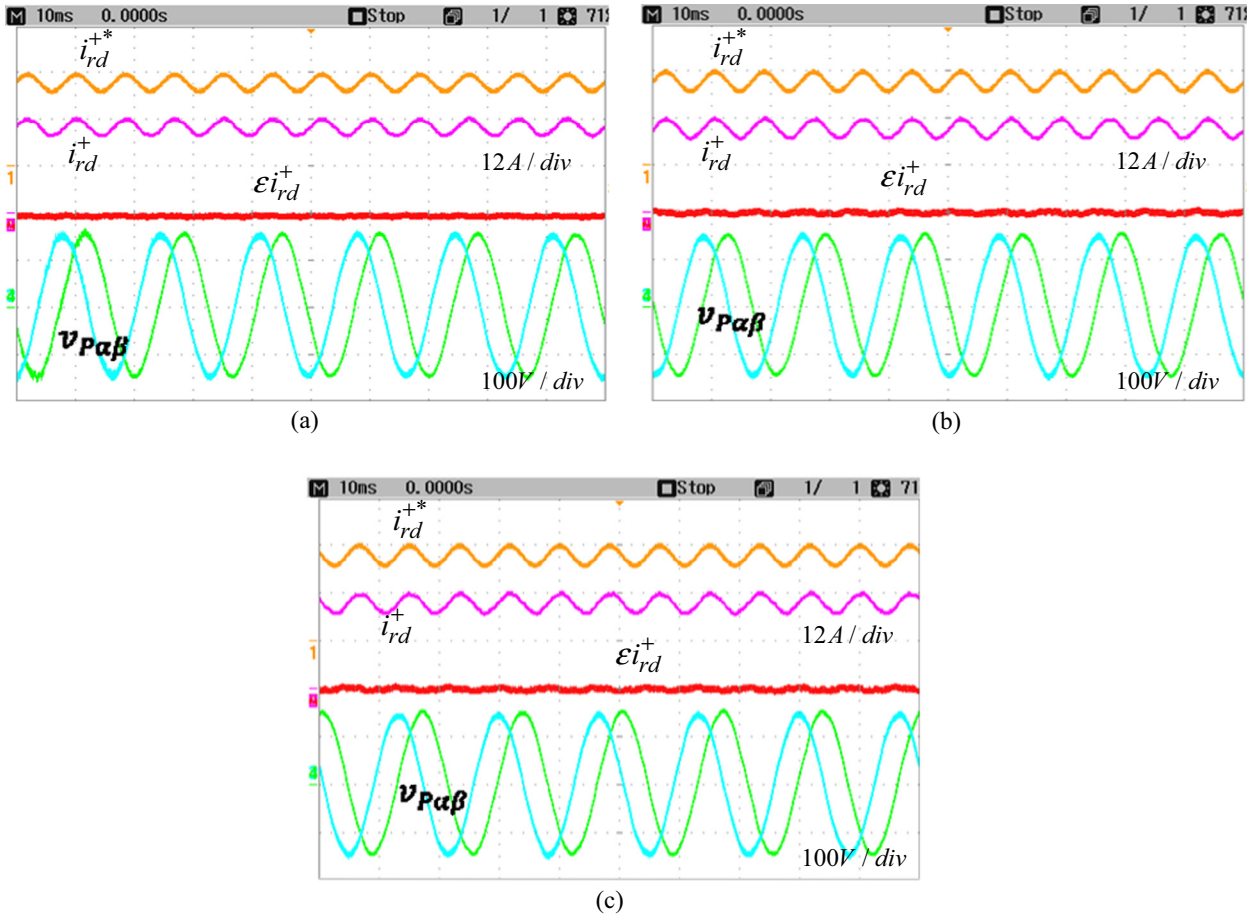

Fig. 14. Control performance of the PCC with variations of mutual inductance L_m: (a) $L'_m = L_m$, (b) $L'_m = 0.7L_m$ and (c) $L'_m = 1.3L_m$.

Downloaded from http://iranpaper.ir
http://www.itrans24.com/landing1.html
سفارش ترجمه این مقاله
آنلاین: www.trans24.ir
تماس: ۶۶۵۷۲۲۳۸-۴۰ (۰۲۱)
trans24

that adequate and precise control of the current controller can be achieved with the proposed PCC approach in the transient response. In contrast, the PIR controller obtains imprecise control due to its insufficient control bandwidth, which results very large current error shown Fig. 12(a). Therefore, the corresponding stator voltage magnitude that is proportional to the rotor current magnitude has similarly low performance. However, due to high control bandwidth of the proposed PCC, the dynamic performance of the stator voltage is faster than the method using the PIR current controller.

In addition, the PCC method is also applicable to variable-speed wind generators. Fig. 13 shows dynamic response of the three-phase rotor current when the rotor speed of the DFIG changes from 1100 rpm (sub-synchronous speed) to 1300 rpm (super-synchronous speed). This result shows that the proposed control scheme is totally robust to the rotor speed variations even through the synchronous speed point.

Finally, the proposed PCC method against the parameter variations is tested. The effect of the generator parameters variation, especially the mutual inductance due to varying temperature and saturation issue in the machine, on the performance of the PCC is tested and shown in Fig. 14. The experimental tests are shown with the regulation performance of the rotor current and the corresponding induced stator output voltages when the value of mutual inductance changes in the range by $\pm 30\% L_m$. As seen, the influence of such parameter variation on the control performance is not considerably, which can be observed at the waveform of three rotor current errors in the steady state. These errors are fully eliminated and their responses are almost identical under the same operating condition. It can be concluded that the proposed PCC method is well controlled with the inductance variation of the DFIG, and therefore the satisfactory performance can be obtained.

Conclusions

In this paper, an improved PCC method to balance the stator voltage for an unbalanced stand-alone DFIG system has been proposed. The proposed predictive control algorithm is developed taking into account the effect of the control time delay. With this compensation method, the actual rotor current is predicted at the end of the current switching period so as to enhance the control performance and accuracy. Based on the discrete DFIG model, the control algorithm predicts the appropriate average rotor voltage vector that eliminates the rotor current error in the next sampling period. The proposed PCC method can precisely regulate both the positive and negative sequence rotor currents without decomposing the measured rotor currents. It is clear from the obtained results that the proposed PCC strategy provides faster and more accurate transient performance compared to the PI and PIR current controllers. Analysis and experimental results have been presented to demonstrate the effectiveness and robustness of the proposed control scheme. Although the results were obtained with the small power scale of 2.2 kW in the lab, the proposed PCC scheme can be totally adopted in higher power DFIG systems to compensate voltage unbalance. High performance DSPs can be used in the current controller so as to increase the switching frequency for higher current control accuracy. However, overall losses in the system due to the high switching frequency have to be considered and analyzed carefully. This would be a great motivation for next further research in high power DFIG based wind turbine systems.

References

[1] Dadhania A, Venkatesh B, Nassif AB, Sood VK. Modeling of doubly fed induction generators for distribution system power flow analysis. Int J Electr Power Energy Syst 2013;53(Dec):576–83.
[2] Xu L, Wang Y. Dynamic modeling and control of DFIG-based wind turbines under unbalanced network conditions. IEEE Trans Power Syst 2007;22(1):314–23.
[3] Zandzadeh Mohammad Jafar, Vahedi Abolfazl. Modeling and improvement of direct power control of DFIG under unbalanced grid voltage condition. Int J Electr Power Energy Syst 2014;59(July):58–65.
[4] Farshadnia Mohammad, Taher Seyed Abbas. Current-based direct power control of a DFIG under unbalanced grid voltage. Int J Electr Power Energy Syst 2014;62(Nov):571–82.
[5] Wong KC, Ho SL, Cheng KWE. Direct control algorithm for doubly fed induction generators in weak grids. IET Electr Power Appl 2009;3(4):371–80.
[6] Zhou P, He Y, Sun D. Improved direct power control of a DFIG-based wind turbine during network unbalance. IEEE Trans Power Electron 2009;24(11):2465–74.
[7] Santos-Martin D, Rodriguez-Amenedo J, Arnalte S. Direct power control applied to doubly fed induction generator under unbalanced grid voltage conditions. IEEE Trans Power Electron 2008;23(5):2328–36.
[8] Shehata EG, Salama Gerges M. Direct power control of DFIGs based wind energy generation systems under distorted grid voltage conditions. Int J Electr Power Energy Syst 2013;53(Dec):956–66.
[9] Abad G, Rodriguez M, Iwanski G, Poza J. Direct power control of doubly-fed-induction-generator-based wind turbines under unbalanced grid voltage. IEEE Trans Power Electron 2010;25(2):442–52.
[10] Rahimi Mohsen, Parniani Mostafa. Low voltage ride-through capability improvement of DFIG-based wind turbines under unbalanced voltage dips. Int J Electr Power Energy Syst 2014;60(Sep):82–95.
[11] Rahimi M, Parniani M. Efficient control scheme of wind turbines with doubly fed induction generators for low-voltage ride-through capability enhancement. IET Renew Power Gener 2010;4(3):242–52.
[12] Banakar H, Luo C, Ooi BT. Steady-state stability analysis of doubly-fed induction generators under decoupled P-Q control. IEE Proc Electr Power Appl 2006;153(2):300–6.
[13] Santos-Martin D, Rodriguez-Amenedo J, Arnaltes S. Providing ride-through capability to a doubly fed induction generator under unbalanced voltage dips. IEEE Trans Power Electron 2009;24(7):1747–57.
[14] Liang J, Qiao W, Harley R. Feed-forward transient current control for low-voltage ride-through enhancement of DFIG wind turbines. IEEE Trans Energy Convers 2010;25(3):836–43.
[15] Zhou Y, Bauer P, Ferreira J, Pierik J. Operation of grid-connected DFIG under unbalanced grid voltage condition. IEEE Trans Energy Convers 2009;24(1):240–6.
[16] Xu L. Coordinated control of DFIG's rotor and grid side converters during network unbalance. IEEE Trans Power Electron 2008;23(3):1041–9.
[17] Pena R, Clare J, Asher G. A doubly fed induction generator using back-to-back PWM converters supplying an isolated load from a variable speed wind turbine. IEE Proc Electr Power Appl 1996;143(5):380–7.
[18] Cardenas R, Pena R, Proboste J, Asher G, Clare J. MRAS observer for sensorless control of standalone doubly fed induction generators. IEEE Trans Energy Convers 2005;20(4):710–8.
[19] Forchetti D, Garcia G, Valla M. Adaptive observer for sensorless control of stand-alone doubly fed induction generator. IEEE Trans Ind Electron 2009;56(10):4174–80.
[20] Iwanski G, Koczara W. DFIG-based power generation system with UPS function for variable-speed applications. IEEE Trans Ind Electron 2008;55(8):3047–54.
[21] Patin N, Monmasson E, Louis JP. Modeling and control of a cascaded doubly fed induction generator dedicated to isolated grids. IEEE Trans Ind Electron 2009;56(10):4207–19.
[22] Pena R, Cardenas R, Escobar E, Clare J, Wheeler P. Control system for unbalanced operation of stand-alone doubly fed induction generators. IEEE Trans Energy Convers 2007;22(2):544–5.
[23] Phan Van-Tung, Lee Hong-Hee. Control strategy for harmonic elimination in stand-alone DFIG applications with nonlinear loads. IEEE Trans Power Electron 2011;26(9):2662–75.
[24] Khatounian F, Monmasson E, Berthereau F, Louis J. Design of an output LC filter for a doubly fed induction generator supplying nonlinear loads for aircraft applications. In: IEEE international symposium on industrial electronics; 2004. p. 1093–98.
[25] Jain A, Ranganathan V. Wound rotor induction generator with sensorless control and integrated active filter for feeding nonlinear loads in a stand-alone grid. IEEE Trans Ind Electron 2008;55(1):218–28.
[26] Kouro S, Cortes P, Vargas R, Ammann U, Rodriguez J. Model predictive control — a simple and powerful method to control power converters. IEEE Trans Ind Electron 2009;56(6):1826–38.
[27] Rodríguez J, Pontt J, Silva C, Correa P, Lezana P, Cortés P, et al. Predictive current control of a voltage source inverter. IEEE Trans Ind Electron 2007;54(1):495–503.
[28] Barrero F, Prieto J, Levi E, Gregor R, Toral S, Duran MJ, et al. An enhanced predictive current control method for asymmetrical six-phase motor drives. IEEE Trans Ind Electron 2011;58(8):3242–52.
[29] Moon Hyung-Tae, Kim Hyun-Soo, Youn Myung-Joong. A discrete-time predictive current control for PMSM. IEEE Trans Ind Electron 2007;43(2):747–59.
[30] Zeng Qingrong, Chang Liuchen. An advanced SVPWM-based predictive current controller for three-phase inverters in distributed generation systems. IEEE Trans Ind Electron 2008;55(3):1235–46.

Downloaded from http://iranpaper.ir
http://www.itrans24.com/landing1.html
سفارش ترجمه این مقاله
آنلاین: www.trans24.ir
تماس: ۶۶۵۷۲۲۳۸-۴۰ (۰۲۱)
trans24

[31] Jeong Se-jong, Song Seung-Ho. Improvement of predictive current control performance using online parameter estimation in phase controlled rectifier. IEEE Trans Power Electron 2007;22(5):1820–5.
[32] Mohamed Y-R, El-Saadany E. Robust high bandwidth discrete-time predictive current control with predictive internal model – a unified approach for voltage-source PWM converters. IEEE Trans Power Electron 2008;23 (1):126–36.
[33] Prodan Ionela, Zio Enrico. A model predictive control framework for reliable microgrid energy management. Int J Electr Power Energy Syst 2014;61 (Oct):399–409.
[34] Vargas R, Rodriguez J, Ammann U, Wheeler PW. Predictive current control of an induction machine fed by a matrix converter with reactive power control. IEEE Trans Ind Electron 2008;55(12):4362–71.
[35] Cortes P, Ortiz G, Yuz JI, Rodriguez J, Vazquez S, Franquelo LG. Model predictive control of an inverter with output LC filter for UPS applications. IEEE Trans Ind Electron 2009;56(6):1875–83.
[36] Drobnic K, Nemec M, Nedeljkovic D, Ambrozic V. Predictive direct control applied to AC drives and active power filter. IEEE Trans Ind Electron 2009;56 (6):1884–93.
[37] Ghijselen JAL, Van den Bossche APM. Exact voltage unbalance assessment without phase measurements. IEEE Trans Power Syst Feb. 2005;20(1):519–20.
[38] Phan Van-Tung, Lee Hong-Hee. Performance enhancement of stand-alone DFIG systems with control of rotor and load side converters using resonant controllers. IEEE Trans Ind Appl Feb. 2012;48(1):199–210.